RESPONSE TO REQUEST FOR ADDITIONAL INFORMATION

04/30/2013

US-APWR Design Certification

Mitsubishi Heavy Industries

Docket No. 52-021

RAI NO.:	**NO. 960-6709 REVISION 3**
SRP SECTION:	**03.07.02 – Seismic System Analysis**
APPLICATION SECTION:	**3.7.2**
DATE OF RAI ISSUE:	**09/24/2012**

QUESTION NO. 3.07.02-216:

Section 4.0 of MHI's TR MUAP-12002 (R0), "Sliding Evaluation and Results," describes the methodology utilized to perform the sliding stability analyses. To assist the staff in evaluating whether the assumptions and modeling approach are consistent with the guidance in SRP Section 3.8.5; and can predict the magnitude of the sliding response, the staff requests the applicant to provide the following additional information:

a) In Section 4.1, "Assumptions," under Assumption number 1, the applicant stated that sliding is assumed to occur in some cases under safe-shutdown earthquake (SSE) but did not identify those cases. The applicant is requested to identify those cases and provide the basis for the assumption.

b) In Section 4.1, under Assumption number 2, the applicant indicated that it is assumed that a small amount of sliding will not modify the ground motion in the vicinity of the basemat. The applicant is requested to provide a quantitative measure of "small amount of sliding." The applicant also stated that, "this assumption is the accepted industry practice for such analyses." The applicant is requested to provide appropriate basis and references to demonstrate the industry practice for such analyses and that it has been accepted by the staff.

c) Regarding the use of the time histories from the SASSI soil-structure interaction (SSI) analyses and applying them in all three directions, the applicant is requested to provide a technical basis and justification for neglecting the rocking motions in relation to the two horizontal axes.

d) Since the soil ground motions from the SASSI SSI analysis is proposed to be used in the lumped-mass stick model (LMSM) sliding stability analysis, the dynamic characteristics between these two models should be consistent or conservative in the LMSM approach. Therefore, the applicant is requested to explain whether the ground motions from the SASSI SSI analyses to be used as input to the LMSM analyses will be based on the embedment case with no connection between the building side wall foundation and the vertical edge of the side soil or based on the connected case. In addition, the applicant is requested to confirm that the two model dynamic characteristics (SASSI and LMSM) are equivalent or that the more conservative ground motion (side soil/wall connection vs. no side soil/wall connection) will be used.

e) Based on the description presented in Sections 4.2.3 and 4.3 of the TR, the subgrade is modeled as a rigid surface and the basemat is modeled as a rigid surface. Contact elements are used between these two surfaces. The applicant is requested to discuss how the effect of dead weight is included in the nonlinear analysis to consider the potential uplift of the basemat; and to provide a technical basis and justification for the sliding stability model and the analysis results.

f) Assumption 4 in the TR indicates that embedment effects (active and passive pressures) are neglected during sliding. The applicant is requested to explain how the effects of surcharge loads due to adjacent structures will be considered in the sliding stability analyses.

g) The applicant in Assumption 5 stated that the maximum ground water level is considered for the sliding analysis. The applicant is requested to justify this assumption and demonstrate that the maximum ground water level case is conservative and will result in the minimum factor of safety (i.e., maximum seismic sliding force and minimum resistance).

h) Assumption 6 in the TR indicates that, "Dynamic soil pressures acting on basement walls before the initiation of sliding are assumed to be compensated by the difference between static and kinetic friction forces acting at the basemat level." Section 4.2.4 of the TR also discusses this item; however, it is not clearly explained. Therefore, the applicant is requested to describe this behavior, explain how the effects of these pressures are considered to be compensated by the difference between static and kinetic friction forces, and describe how this assumption is conservative and will be demonstrated, as stated in Section 4.2.4 of the TR.

ANSWER:

This answer revises and replaces the previous MHI answer that was transmitted by Letter UAP-HF-12292 (ML12356A069).

a) Assumption #1 has been removed from Technical Report MUAP-12002, Rev. 1. The intent of the Technical Report is to implement analysis methodologies where sliding is allowed to occur.

b) There are two basic methodologies generally accepted by the industry practice for nonlinear sliding analysis (a comprehensive review is presented in Reference 1):

    1) The decoupled method (e.g., References 2, 3), which uses a dynamic analysis based on displacement continuity (i.e., no sliding allowed) to calculate the equivalent seismic loading throughout the structure, and a second analysis in which the equivalent load time history is used to calculate the seismic induced sliding.

    2) The fully coupled method (e.g., References 4 to 6) that captures in one single analysis the dynamic response of the sliding mass and the nonlinear stick-slip sliding response at the interface with the subgrade.

    The effect of the methodology for nonlinear sliding analysis on the calculated sliding was investigated by a series of authors. Based on these studies it was concluded that the decoupled approximation provides, in general, conservative results. More recent studies concluded, however, that decoupled analyses may provide under-conservative results for certain situations involving systems with low values of the yield acceleration and high characteristic periods.

The non-linear sliding analysis used by MHI is a combination of decoupled and fully coupled analyses. The calculation is performed in two steps: The first step, assuming displacement continuity, provides the base input acceleration for the second step. The second step is a coupled analysis, in that the dynamic response of the structure and the nonlinear sliding are captured in a single analysis. It is therefore expected that the results, in terms of sliding, obtained by the MHI method would range between the results of a decoupled and a fully coupled analysis. It will be demonstrated in the following that, for the specific structural characteristics of the reactor building (R/B) complex and the frequency characteristics of the seismic input motions used for sliding analysis, the decoupled analysis yields results that are either conservative (i.e., larger sliding) or similar to the ones produced by a fully coupled sliding analysis, and therefore the method used by MHI, which is a combination of the decoupled and the fully coupled methods, does not produce under-conservative results in terms of sliding.

Bray and Rathje (2000), Reference 7, present the results of a parametric study on the effect of analysis method on calculated sliding. The study covers a large range of parameters, including:

- Threshold acceleration ratio, k_y/k_{max}, ranging between 0.05 and 0.9, where $k_y g$ is the inertial coefficient corresponding to a pseudo-static factor of safety for sliding equal to one and $k_{max}g$ is the maximum earthquake acceleration in the plane of sliding (g is the acceleration of gravity).

- Period ratio, T_s/T_m ranging between zero and 5, where T_s is the fundamental period of the sliding mass, and T_m is the fundamental period of the earthquake ground motion (defined in equation (1) of Reference 7).

- Total sliding between 0.1cm (0.04in) and 100cm (40in).

The study presented in Reference 7 was originally intended for sliding earth masses. However, the range of parameters addressed in the study is large and includes characteristics corresponding to building structures. It will be demonstrated that this range also includes the parameters used in the nonlinear sliding analyses of the US-APWR standard plant structures. Moreover, the nonlinear sliding analysis method used by MHI is a combination of the two methods compared in the study. Therefore, this study is relevant for discussing the effect of sliding analysis method on the computational results.

The values corresponding to the parameters in used in Reference 7 are as follows (values calculated for the R/B complex, subgrade profile 900-200, input acceleration time history Nahanni - that resulted in the largest sliding):

1) Maximum horizontal acceleration in a horizontal plane:

$$k_{max} = \frac{1}{g}\max_t \sqrt{a_x^2(t) + a_y^2(t)} = 0.35 \quad (1)$$

2) Threshold acceleration:

$$k_y = \frac{\mu(Mg - U - F_{Iv})}{Mg} = 0.22 \quad (2)$$

With: M = mass of the R/B complex, U = 0.262Mg - Buoyant force considered in sliding analyses, F_{Iv} = Mga_v - the vertical force of inertia calculated for a_v = 0.3.

3) Calculated sliding: δ = 0.637in

4) Fundamental period of the structure with cracked concrete section: T_s^{CR} = 0.25sec - corresponding to a fundamental frequency of 4Hz that includes approximately 20-percent of the total modal mass (see Figure 5.2.2.2-1 in Technical Report MUAP-12002, Rev. 1). The corresponding value for the structure with uncracked section is T_s^{UC} = 0.15sec (Figure 5.2.2.2-5 of Technical Report MUAP-12002, Rev. 1).

5) Mean period of the earthquake ground motion, calculated using equation (1) in Reference 7, T_m = 0.63sec (average from T_{mx} = 0.62sec and T_{my} = 0.64sec - from the input accelerations in two horizontal directions).

The parameters of the R/B complex relevant to the parametric study are:

- Threshold acceleration ratio: k_y/k_{max} = 0.63

- Period ratio: T_s/T_m = 0.25/0.62 = 0.4 (for the cracked section) and T_s/T_m = 0.15/0.62 = 0.24 (for the uncracked section)

The parametric study results are presented in terms of these two parameters in Figures 10c and 12a of Reference 7, that are reproduced here as Figures 1 and 2, respectively. The markings in red indicate results corresponding to R/B complex with cracked and uncracked section.

As seen in Figure 1, for the parameters corresponding to the R/B complex (and indicated by red arrows) the decoupled analysis is either slightly conservative or provided close results to the coupled analysis. Figure 2 shows close match between the results of decoupled and coupled analyses for the threshold acceleration ratio corresponding to the R/B complex.

The parameters relevant to the study and used in Figures 1 and 2 (namely k_y/k_{max} and T_s/T_m) have been calculated for all subgrade profiles and all input acceleration time histories. The ranges of these parameters for the rock profiles (900-200, 900-100 and 2032-100) that dominate sliding are:

- Between 0.52 and 0.64 - for k_y/k_{max}

- Between 0.24 and 0.47 for T_s/T_m

These ranges are shown by blue shaded areas in Figures 1 and 2, and support the conclusion that, for the range of parameters used in the MHI sliding analyses, the decoupled method provides similar or slightly conservative results in terms of sliding as compared to the fully coupled method.

REFERENCES

1. Bray J.D. (2007). Simplified seismic slope displacement procedures. Chapter 14 in *Proc. Earthquake Geotech. Eng., 4th Int. Conf. on Earthquake Geotech. Eng. - Invited Lectures*, K.D. Pitilakis, ed., Vol. 6, Springer, New York, p. 327-353.

2. Makdisi, F. and Seed, H. (1978). Simplified procedure for estimating dam and embankment earthquake-induced deformations, *J. Geotechnical Engineering, ASCE*, 104(7):849-867.
3. Bray J.D., Rathje, E.M., Augello, A.J. and Merry, S.M. (1998). Simplified seismic design procedures for geosynthetic-lined, solid waste landfills. *Geosynthetics International*, 5(1-2):203-235.
4. Chopra, A.K. and Zhang, L. (1991). Earthquake-induced base sliding of concrete gravity dams. *J. Structural Engineering*, *ASCE*, 117(12):3698-3719.
5. Rathje, E.M. and Bray, J.D. (1999). An examination of simplified earthquake-induced displacement procedures for earth structures. *Canadian Geotechnical J.*, 36:72-87.
6. Bray, J.D. and Travasarou, T. (2007). Simplified procedure for estimating earthquake-induced deviatoric slope displacement. *J. Geotechnical and Geoenvironmental Eng., ASCE,* 133(4):381-392.
7. Rathje, E.M. and Bray, J.D. (2000). Nonlinear coupled seismic sliding analysis of earth structures. *J. Geotechnical and Geoenvironmental Eng., ASCE,* 126(11):1002-1014.

Figure 1. Displacement difference between decoupled and coupled analysis versus T_s/T_m, for k_y = 0.2 (modified after Figure 10c of Reference 7)

Figure 2. Displacement difference between decoupled and coupled analysis versus k_y/k_{max}, for T_s/T_m = 0.5 (modified after Figure 12a of Reference 7)

c) Based on the results of sensitivity analyses performed for the reactor building R/B complex shown in Section 5.2.1.1 of Technical Report MUAP-12002, Rev. 1, and for the turbine building (T/B) shown in Section 5.3.1.1 of MUAP-12002, Rev. 1, it was concluded that input rocking motion with respect to the two horizontal axes may be important for the results of nonlinear sliding analysis. Therefore, rocking input in relation to the two horizontal axes is applied in the nonlinear sliding analysis. The rocking motion is extracted from the results of soil-structure interaction (SSI) analyses performed with SASSI and is applied as rotational accelerations about the two horizontal axes. More details regarding derivation of these rotational accelerations are presented in Section 4.5.2 of the Technical Report MUAP-12002, Rev. 1.

d) As stated in Section 4.2.2 of Technical Report MUAP-12002, Rev. 1, the models used in the nonlinear sliding analysis were taken from Technical Report MUAP-10006, Rev. 3, and Technical report MUAP-11002, Rev. 2. The basement structural elements and free field soils are connected to include near field backfill, see Section 03.3.1 in Technical Report MUAP-10006, Rev. 3. Therefore the ground motions from the SASSI SSI analyses used as input for the nonlinear sliding analyses are based on the fully bonded model. Figures 03.3.4.1-1 through 03.3.4.2-3 of Technical Report MUAP-10006, Rev. 3, provides a visual representation of this fully bonded connection.

The dynamic characteristics of the SASSI model and lumped-mass-stick model are comparable. The validation and calibration of the lumped-mass-stick model was performed as described in Section 4.3 and Appendix A of Technical Report MUAP-12002, Rev. 1.

e) The dead weight is included in the nonlinear sliding analysis through the mass of continuous elements used to model the basement and the concentrated masses modeling the superstructure. These masses accurately reproduce the actual masses in the finite element (FE) Model. The dead weight is reduced by the uplift force (due to groundwater), applied as an upward vertical pressure acting on the basemat.

The possibility of uplift is captured by the numerical model through the use of compression-only contact elements with finite stiffness as explained in Section 4.2.3 of the Technical Report MUAP-12002, Rev. 1. To illustrate the manner in which uplift is captured by the numerical model, figures with contours of calculated pressures at the basemat-subgrade interface, showing uplift (areas with zero pressure) during seismic shaking, are presented in Attachment 2 (A2) of this RAI Response.

The contours are from the nonlinear sliding analysis performed with ANSYS and using the full FE model for the reactor building (R/B) complex structure with cracked concrete section properties placed on subgrade profile 900-200 and acted by the Nahanni acceleration time history (this is the case that produced maximum sliding). The computed sliding in the X and Y directions, along with the time instants selected for plotting pressure contours, are shown in Figure A2-1 of Attachment 2. The contours of pressure at the basemat-subgrade interface for the three time instants are presented in Figures A2-2 through A2-4. The three time instants have been selected as follows: Time = [ ] seconds (Figure A2-2) - during strong shaking, with no sliding and some uplift; Time = [ ] seconds (Figure A2-3) - during strong shaking, starting sliding and maximum uplift; Time = [ ] seconds (Figure A2-4) - during weaker shaking, no sliding and no uplift; The dark blue contours shown in Figures A2-2 and A2-3 indicate uplift (the pressure on the contact elements is zero).

f) The reason for neglecting embedment effects, i.e., active and passive pressures, for a four-sided embedded structure and an explanation that this assumption is conservative are provided in Section 4.5.3 of Technical Report MUAP-12002, Rev. 1. The effect of adjacent structures on lateral earth pressures is discussed below.

The surcharge loads from adjacent structures are acting as driving forces for sliding in the active state or in the at-rest state (passive reactions oppose sliding and therefore it is conservative to ignore any additional passive reactions in the sliding analysis). The following Standard Plant structures may affect lateral earth pressures from embankment acting on the below-grade walls of the R/B complex:

- T/B: The below grade North wall of this structure is placed at a distance of 20 ft - 6 in. from the below grade South wall of the R/B complex (refer to Section 3-3 in Attachment 1 of the response to Question 03.07.02-212). This distance is larger than the difference between the basemat elevations of the R/B complex and the T/B (namely 15 ft-1 in.), and therefore presence of the T/B does not increase the active or at-rest lateral earth pressures acting on the R/B complex wall.

- Access Building (AC/B). This structure is placed near the West wall of the auxiliary building (A/B), with a 16 inch gap filled with backfill (refer to the Plane View and to Section 2-2 in Attachment 1 of the response to Question 03.07.02-

212). As calculated in Attachment 3 (A3) of this RAI Response, the vertical pressure at the basemat elevation of the AC/B due to its weight is smaller than the vertical effective stress in the embankment at basemat elevation in the absence of the structure, and therefore this structure does not have any negative effect on the sliding stability of the R/B complex.

- Tank house. This structure is placed near the North wall of the AC/B, with a 16 in. gap filled with backfill (refer to the Plan View and to Section 1-1 in Attachment 1 of the response to Question 03.07.02-212). The additional forces per unit length of wall due to the presence of the tank house are calculated in Attachment 3 of this RAI Response, and are: additional active thrust, ΔP_a^{TH} = 2.6 kip/ft, and additional at-rest thrust, ΔP_0^{TH} = 5 kip/ft.

The effects of these additional forces on sliding are discussed in the following for two situations:

Case 1: No sliding. In this case the forces that are neglected in the nonlinear sliding analysis are: (1) the dynamic pressure, having a maximum value of F_D = 49,435 kips and calculated as discussed in Section 5.2.1.3 of Technical Report MUAP-12002, Rev. 1, and (2) the additional at rest thrust from the tank house ($\Delta F^{TH} = L_{TH} \times \Delta P_0^{TH}$ = 620 kips). L_{TH} = 124 ft is the length of the tank house, as shown in the Plan View in Attachment 1 of the response to Question 03.07.02-212. As discussed in Section 5.2.1.3 of Technical Report MUAP-12002, Rev. 1, the reserve resistance force at the basemat for considering the kinetic friction coefficient in the sliding analysis when the structure does not slide is 81,584.8 kips, which is larger than the sum $F_D + \Delta F^{TH}$, representing forces neglected during non-sliding sequences.

Case 2: During sliding. In this case the force that is neglected in the nonlinear sliding analysis is the additional active thrust from the tank house, ΔP_a^{TH} = 2.6 kip/ft (see Attachment 3 of this RAI Response). This force is in addition to the active thrust acting on the active wall of the R/B complex (i.e., the wall moving away from the surrounding backfill): P_a = 30.1 kip/ft, calculated in Attachment 3. The force acting on the passive wall (i.e., the wall moving towards the surrounding backfill) is at least as large as the force resulting from pressure at rest, P_0 = 55.8 kip/ft, calculated in Attachment 3. From the values discussed above, the force acting on the active wall (i.e., $P_a + \Delta P_a^{TH}$) is smaller than the resisting force acting on the passive wall, and therefore it is conservative to neglect the pressures from embankment in the sliding analysis.

Any effects on embankment pressures from nearby non-standard plant structures will be addressed by the Combined License (COL) Applicant on a site specific basis.

g) This assumption has been verified, in terms of calculated seismic induced sliding displacement, through sensitivity analyses performed with the validated lumped-mass-stick model of the R/B complex with cracked concrete section properties. The sensitivity analyses have been performed for all six subgrade profiles and all five seismic acceleration time histories and are described in more detail in Appendix B.1.2 of Technical Report MUAP-12002, Rev. 1. In summary, a lowering of the groundwater level from one foot below grade to 20 feet below grade resulted in a significant reduction, i.e., generally 50-percent or more, in displacement for all five time histories and all six subgrade profiles. In some cases lowering the ground water level to 20 feet below grade resulted in no sliding.

h) Technical Report MUAP-12002, Rev. 1, describes in detail how the effects of dynamic soil pressures acting on the basement walls, before the initiation of sliding, are compensated by the difference between static and kinetic friction forces. The explanation is based on quantitative force analysis and is described in Sections 5.2.1.3 and 5.3.1.3 of Technical Report MUAP-12002, Rev. 1, for the R/B complex and for the T/B, respectively.

Impact on DCD

There is no impact on the DCD.

Impact on R-COLA

There is no impact on the R-COLA.

Impact on S-COLA

There is no impact on the S-COLA.

Impact on PRA

There is no impact on the PRA.

Impact on Technical/Topical Report

There is no impact on the Technical/Topical Report.

This completes MHI’s response to the NRC’s question.

ATTACHMENT 2 - Modeling Uplift during Nonlinear Sliding Analysis

For RAI 960-6709, Question 03.07.02-216(e)

Figure A2-1. Sliding analysis results using the FE model of the R/B Complex with cracked concrete section properties for subgrade profile 900-200 and Nahanni acceleration time history. The time instants for basemat pressure contours are indicated by arrows.

Figure A2-2. Pressure contours at basemat-subgrade interface calculated at Time = 6.8 seconds during nonlinear sliding analysis of the R/B Complex with cracked concrete section, for subgrade profile 900-200 and Nahanni acceleration time history. Dark blue color indicates uplift.

Figure A2-3. Pressure contours at basemat-subgrade interface calculated at Time = 9.5 seconds during nonlinear sliding analysis of the R/B Complex with cracked concrete section, for subgrade profile 900-200 and Nahanni acceleration time history. Dark blue color indicates uplift.

Figure A2-4. Pressure contours at basemat-subgrade interface calculated at Time = 14 seconds during nonlinear sliding analysis of the R/B Complex with cracked concrete section, for subgrade profile 900-200 and Nahanni acceleration time history.

ATTACHMENT 3 - Effect of Adjacent Structures on Lateral Earth Pressures acting on the R/B Complex

For RAI 960-6709, Question 03.07.02-216(f)

The lateral earth pressures from embankment acting on the below grade walls of the R/B Complex and accounting for surcharges from adjacent structures are schematically presented in Figure A3-1. The pressures are marked by lower case letters and the thrust forces per unit length of wall are marked by upper case letters. For the cases of interest here (Case 1 - no sliding, and Case 2 - sliding, discussed in the answer to Question 03.07.02-216(f) of this RAI), the notations in Figure A3-1 are as follows:

- $\Delta\sigma_v$ is the additional vertical pressure due to the adjacent structure
- Δp is the additional horizontal pressure induced by the adjacent structure
- P is the active (P_a) or at rest (P_0) thrust per unit length of wall acting in the absence of the adjacent structure
- ΔP is the additional active (ΔP_a) or at rest (ΔP_0) thrust per unit length of wall due to the adjacent structure
- P_E is the embankment pressure acting on the opposite side of the R/B Complex with respect to the adjacent structure

The other symbols in Figure A3-1 are as follows:

- H = 42'-3" is the embedment depth of the R/B Complex
- H_1 is the embedment depth of the adjacent structure (H_1 = 33'-11" for the AC/B and H_1 = 16'-2" for the tank house)
- $\Delta H = H - H_1$ (ΔH = 26'-1" for the tank house)

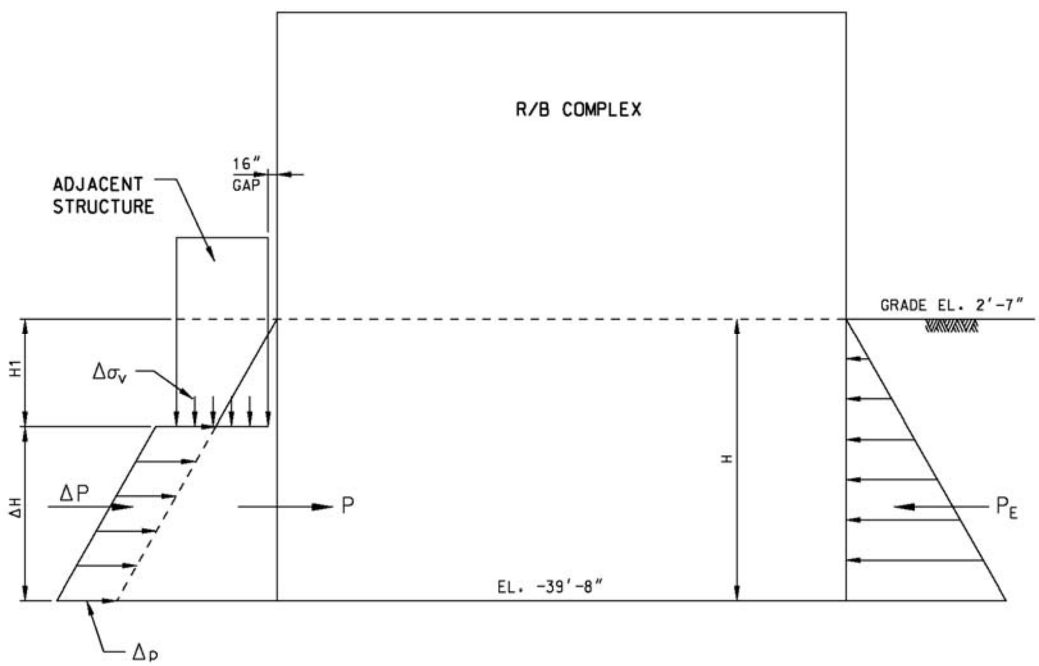

Figure A3-1 Effect of adjacent structures on lateral earth pressures acting on the below-grade walls of the R/B Complex

Assumptions:

1. The groundwater level is below the R/B Complex basemat level (this is conservative, as presence of groundwater reduces the effective lateral earth pressures).
2. Rankine's theory of lateral earth pressure is used throughout, with coefficient of active pressure, $k_a = 0.27$, and coefficient of lateral pressure at rest, $k_0 = 0.5$.

The additional vertical pressure due to the adjacent structure, $\Delta\sigma_v$ is calculated as follows:

- For the AC/B: $\Delta\sigma_v = W_{ACB} / (L_{ACB} \times B_{ACB}) - \gamma \times H_1 = -1.2$ ksf < 0 (W_{ACB} = 28,000 kips is the weight; $L_{ACB} \times B_{ACB}$ = 165' x 56' are the dimensions in a horizontal plane; γ = 125pcf is the in-situ unit weight of the backfill).
- For the tank house: $\Delta\sigma_v = W_{TH} / (L_{TH} \times B_{TH}) - \gamma \times H_1 = 0.37$ ksf (W_{TH} = 16,000 kips is the weight and $L_{TH} \times B_{TH}$ = 124' x 54' are the dimensions in a horizontal plane).

The vertical stress induced by the AC/B at its basemat (3.03ksf) is smaller than the vertical effective stress in the embankment at that elevation (4.24 ksf), therefore this structure does not produce any increase in lateral earth pressures acting on the R/B Complex. The forces from lateral embankment pressure for the tank house are as follows:

Case 1: No sliding.

$\Delta p = k_0 \, \Delta\sigma_v = 0.19$ ksf;

$\Delta P_0^{TH} = \Delta p \, \Delta H = 5$ kip/ft;

$P_E \geq P_0 = ½ \, k_0 \, \gamma \, H^2 = 55.8$ kip/ft

Case 2: Sliding.

$\Delta p = k_a \, \Delta\sigma_v = 0.1$ ksf;

$\Delta P_a^{TH} = \Delta p \, \Delta H = 2.6$ kip/ft;

$P_a = ½ \, k_a \, \gamma \, H^2 = 30.1$ kip/ft